The behavior of a cavitation bubble near a rigid wall

Sheguang Zhang* and James H. Duncan
Department of Mechanical Engineering, The University of Maryland
College Park, MD 20742

and

Georges L. Chahine
DYNAFLOW, INC. *7210 Pindell School Road,*
Fulton, MD 20759

Abstract. During the collapse of an initially spherical cavitation bubble adjacent to a rigid wall, a wall-directed re-entrant jet forms from the side of the bubble farthest from the wall. This jet eventually impacts with the bubble surface closest to the wall (jet-liquid impact) and penetrates into the fluid adjacent to the wall. The bubble behavior associated with this process is investigated numerically using a boundary element method developed by Zhang, Duncan and Chahine (1993). The results show that the jet-liquid impact creates a ring-shaped bubble. A shear layer is generated along the impact interface. In the numerical model this shear layer is modeled as a vortex sheet. The impact also generates circulation and impulsive pressures in the flow system.

Key words: Bubble Collapse, Jet-liquid Impact, Boundary Integral Method.

1 Introduction

Experimental investigations of the behavior of a cavitation bubble near rigid boundaries (Tomita and Shima (1986); (Vogel *et al.*, 1989) have shown that, as the bubble collapses, its shape becomes nonspherical and a wall-directed re-entrant jet is formed from the side of the bubble farthest from the wall. Eventually, the re-entrant jet impacts with the opposite side of the bubble and penetrates into the slower-moving fluid close to the wall. Corresponding numerical simulations with boundary integral methods have also shown the formation and motion of the re-entrant jet during bubble collapse (Blake, et al. (1986); Chahine and Perdue (1988); Duncan and Zhang (1991)). However, these simulations could not proceed past the time where jet-liquid impact occurs. To explore the bubble evolution after the initial impact, Best (1993) employed a two-step procedure to simulate the transition of a simply connected bubble shape to a ring bubble shape assuming that the jet-liquid takes place at a single point on the bubble surface at one instant in time. Zhang, Duncan and Chahine (1993) have also developed a boundary integral method for treating the final stage of the collapse of a bubble near a rigid wall. In this method, the jet-liquid impact occurs continuously over a short period of time and generates a shear layer along the impact interface. The present paper presents some aspects of the bubble behavior as computed by the model of Zhang et al. (1993).

* Present address: The Department of Ocean Engineering, MIT, Cambridge, MA 02139

J. R. Blake et al. (eds.), Bubble Dynamics and Interface Phenomena, 429–436.

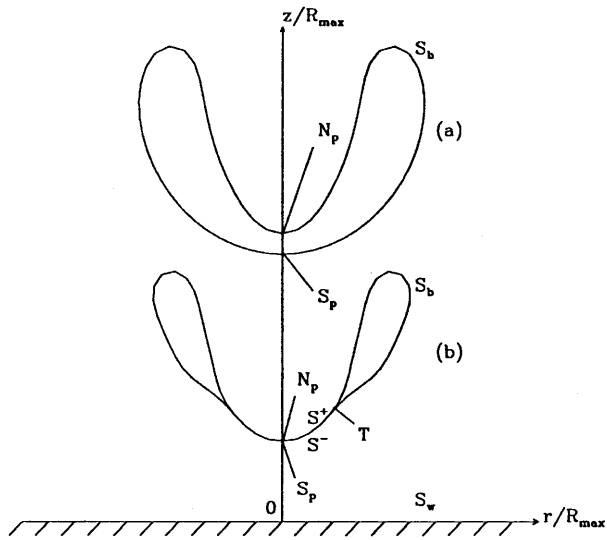

Fig. 1. A cylindrical coordinate system and two sketches of axisymmetric bubble profiles corresponding to two different stages during a bubble evolution: (a) before and (b) during a re-entrant jet penetration. S_b represents a regular surface, S^+ and S^- comprise a common surface which is connected to S_b at the triple point T, and S_w denotes an infinite rigid wall.

2 Theory and numerical procedures

A cavitation bubble axisymmetrically growing and collapsing near a rigid wall is simulated with potential flow theory and a boundary integral method. A cylindrical coordinate system is used to describe the fluid motion. A schematic showing of the two stages of the bubble collapse, before impact and during impact, is given in Figure 1. A rigid wall is located in the plane $z = 0$ and extends to infinity. The pressure in the fluid far from the bubble, P_∞, is maintained constant as is the pressure in the bubble, P_0. Before initial impact, the bubble surface, as shown in Figure 1(a), is entirely a regular surface and the fluid domain, D, is a simply-connected region bounded by the bubble surface, S_b, the rigid wall, S_w, and an imaginary boundary at infinity, S_∞. After initial impact, S_b is transformed into an irregular surface as shown in Figure 1(b). This surface consists of two different regions: a common surface region which is comprised of the two surfaces S^+ and S^-, representing the vortex sheet, and a regular surface region, S_b, which includes the ring bubble. The fluid domain is still simply-connected when the internal boundary is taken as the union of S_b, S^+ and S^-. The length scale for the problem is taken as R_{max}, (the maximum radius the bubble would have achieved

in an infinite fluid), the time scale is taken as $R_{max}\sqrt{\rho/(P_\infty - P_0)}$, (the collapse time of a spherical bubble in an infinite fluid of density ρ), and the pressure scale is $P_\infty - P_0 = \Delta P$. The quantities appearing in the remainder of the paper are non-dimensionalized with respect to these three parameters.

The governing equation for the velocity potential with $\vec{u} = \nabla\phi$ is Laplace's equation,

$$\nabla^2\phi(\vec{x},t) = 0, \quad \vec{x} \in D, \tag{1}$$

where $\vec{x}$ is the spatial coordinate. The initial condition is defined by Rayleigh's theory (Blake, et al 1984). At infinity, there is no motion of the fluid and on the rigid wall the normal velocity of the fluid is zero. The boundary conditions following a fluid particle $\vec{p}$ on S_b, are the kinematic condition,

$$\frac{d\vec{x}_p}{dt} = \nabla\phi(\vec{x}_p,t), \tag{2}$$

and the dynamic condition,

$$\frac{D\phi}{Dt} = \frac{1}{2}|\nabla\phi|^2 + \frac{P_\infty - P_0}{\rho}, \tag{3}$$

where $\vec{x}_p$ is the position vector of the particle $\vec{p}$. After the initial impact, the boundary conditions on $S^+ \cap S^-$, must be introduced. The normal velocity across the interface is assumed to be continuous and is given by

$$\frac{d\vec{x}_p^n}{dt} = \frac{\partial\phi}{\partial n_p}\vec{n}_p, \tag{4}$$

where $\vec{n}_p$ is the unit normal vector at $\vec{p}$ on S^+ and $\vec{x}_p^n$ is the projection of $\vec{x}_p$ in the direction $\vec{n}_p$. The continuity of the pressures across $S^+ \cap S^-$ requires

$$\frac{D(\phi^+ - \phi^-)}{D_n t} = -\frac{1}{2}\left[(\frac{\partial\phi^+}{\partial s^+})^2 - (\frac{\partial\phi^-}{\partial s^-})^2\right], \tag{5}$$

which is derived from Bernoulli's equation. In this equation, s^+ and s^- are the arclength coordinates on S^+ and S^- respectively and D/D_n indicates that the time derivative is carried out following the normal motion of the fluid particles on S^+.

In the numerical technique, a boundary integral method is used to solve Laplace's quation in an Eulerian frame and then, the fluid particles and the value of ϕ on the bubble surface are advanced in time by a Lagrangian scheme. The geometry of the bubble is discretized by a set of ring-shaped panels and the coordinates r and z are interpolated with the cubic spline technique; the field functions ϕ and $\partial\phi/\partial n$ in each panel are interpolated in terms of linear functions of the panel

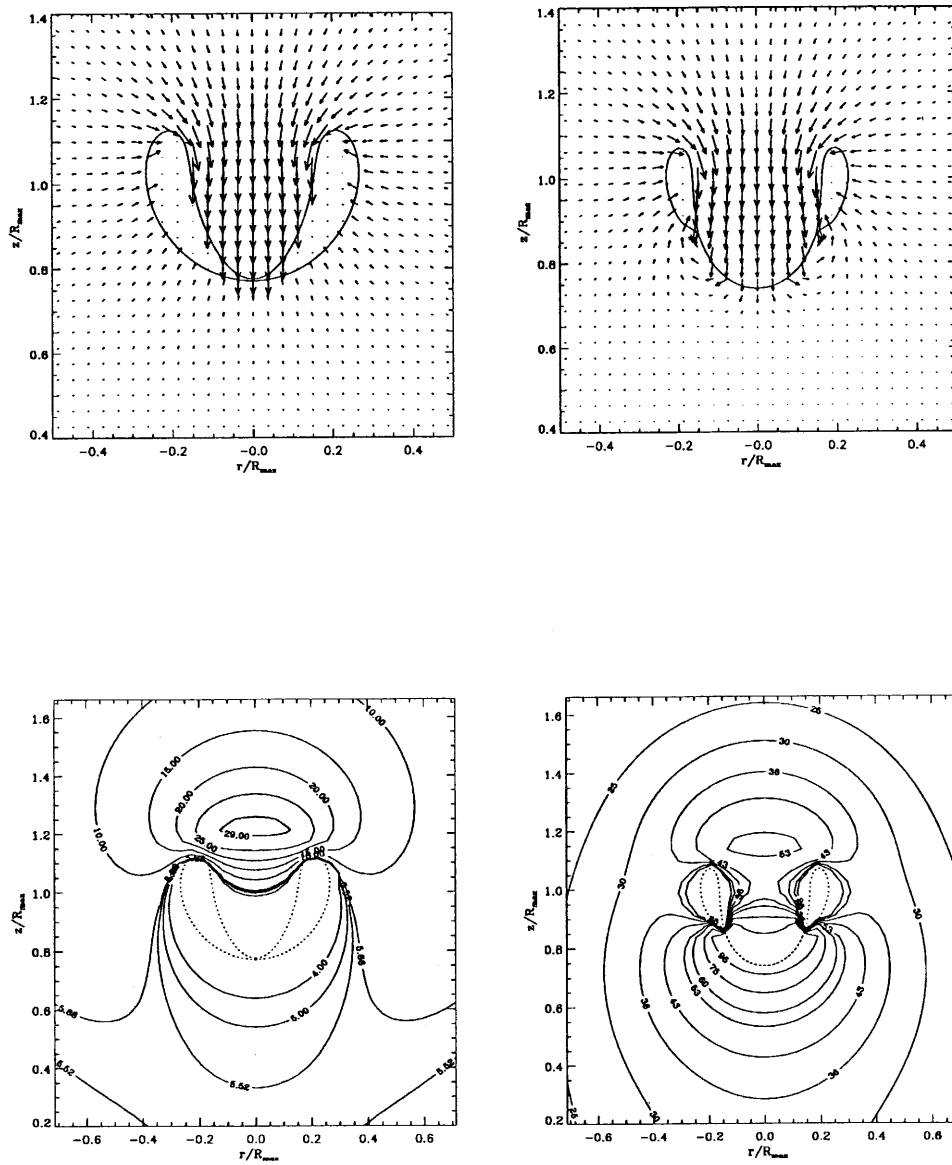

Fig. 2. Bubble profiles, velocity fields and pressure contours for $Z_0 = 1.5$ and $R_0 = 0.1$ at $t = 2.08545$ for (a) and (c), and at $t = 2.09241$ for (b) and (d). The lengths of the vectors are scaled to the maximum velocity. The bubble profiles are shown as a dotted lines.

arclength s. The algebraic equation system formed by discretizing the boundary integral equations are solved at each time step. Once the field equations are solved, a predictor-corrector scheme with variable time steps is adopted to integrate the boundary conditions (2) and (3) for the case of before the initial impact and (2), (3), (4) and (5) for the case of after the initial impact. Thus, the new bubble profiles $S_b \cup S^+ \cup S^-$ and the new boundary conditions for ϕ on S_b and $\phi^+ - \phi^-$ on S^+ can be specified at the next time step. The details of the theory and numerical scheme can be found in Zhang, et al (1993).

3 Results and discussions

The bubble profiles, velocities and pressures at a time just before the impact and at a time during the impact are presented in figure 2 for $Z_0 = 1.5$ and in figure 3 for $Z_0 = 1.1$, respectively. As shown in figure 2 (a) and figure 3 (a), just before the initial impact the re-entrant jet is moving toward the wall while the fluid underneath the surface opposite to the jet is moving away from the wall. After the initial impact the bubble is transformed into a ring bubble attached to an impact interface as plotted in figure 2 (b) and figure 3 (b) with $Z_0 = 1.5$ and 1.1, respectively. The impact interface in each of the two plots represents a shear layer which is modeled as a vortex sheet. It can be seen from the plots that after the initial impact, the jet is still directed toward the wall but the speed of the jet is reduced significantly in comparison with the speed just before impact.

Corresponding to the bubble profiles and velocities in Figures 3 (a) and (b), the pressure contours at the same instants are presented in figures 2 (c) and (d), respectively. The important features in the pressure distribution are the generation of a high pressure region around the impact interface due to the drastic change in fluid inertia during the impact.

Before initial impact, the circulation is zero for any closed path within the fluid. However, after initial impact, any closed path that crosses the vortex sheet will have a non-zero circulation. Figure 4 shows the circulation versus time after initial impact for two separate integration paths. The first path starts at $r = 0$ on the bottom side of the vortex sheet, extends over the bottom of the vortex sheet and around the ring bubble and ends at $r = 0$ on the top side of the vortex sheet. The circulation for this path is called Γ_{ns} and is equal to $\phi_{np} - \phi_{sp}$, where ϕ_{np} and ϕ_{sp} are the values of ϕ at $r = 0$ on the top and bottom, respectively, of the vortex sheet. From Equation (5), it can be seen that Γ_{ns} is constant after initial impact. The second path goes around the ring bubble, starting and ending at the triple point. The circulation for this path, Γ_r, is the circulation associated with the ring bubble and $\Gamma_r = \phi_T^+ - \phi_T^-$. At the time of intial impact, $\Gamma_r = \Gamma_{ns}$. Curves of Γ_{ns} and Γ_r are given in Figure 4 for four values of Z_0 (1.75, 1.5, 1.25 and 1.1). As can be seen from the figure Γ_{ns} increases with decreasing Z_0. The circulation of the ring bubble continually decreases with time after initial impact reaching as little as 50% of Γ_{ns} at the end of the calculation. This behavior is quite different than

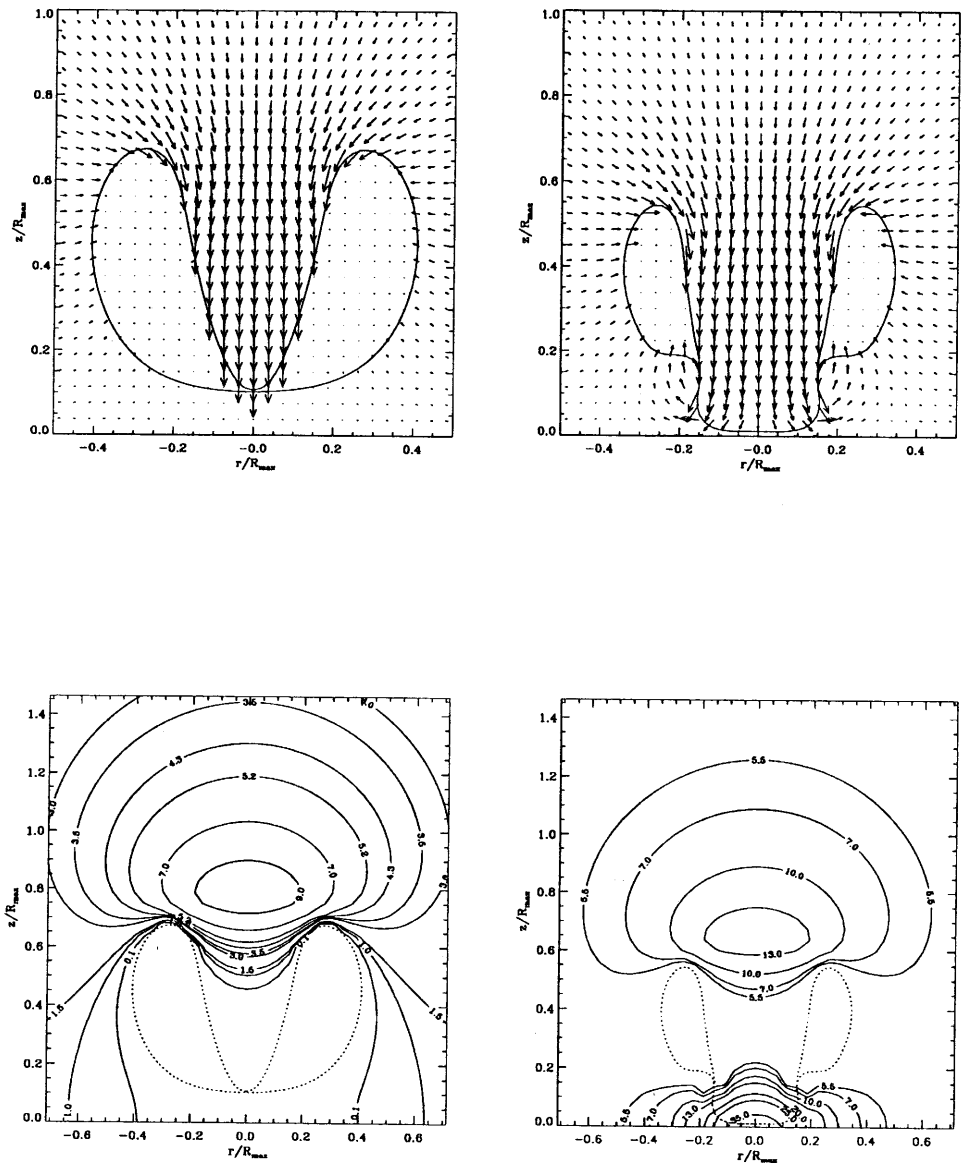

Fig. 3. Bubble profiles, velocity fields and pressure contours for $Z_0 = 1.1$ and $R_0 = 0.1$ at $t = 2.15059$ for (a) and (c), and at $t = 2.18074$ for (b) and (d). The lengths of the vectors are scaled to the maximum velocity. The bubble profiles are shown as a dotted lines.

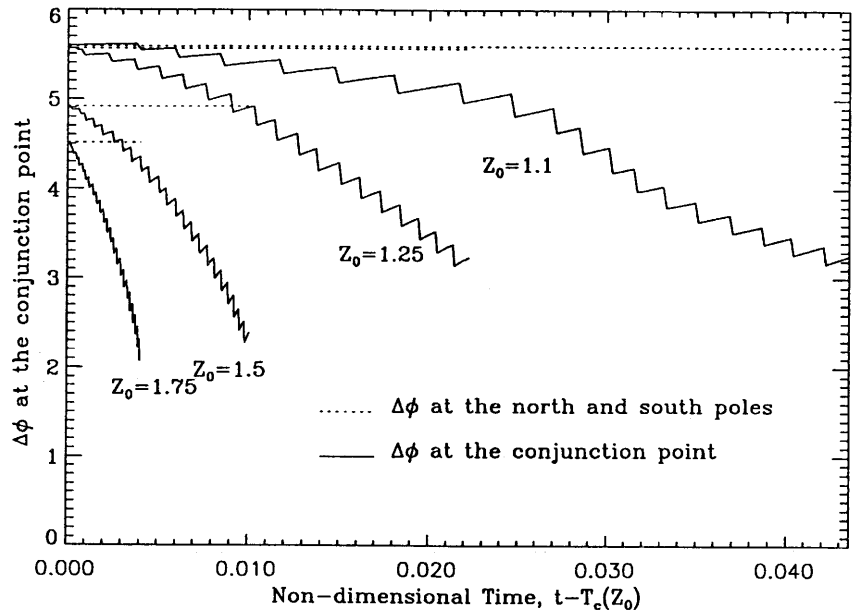

Fig. 4. The total circulation, $\Gamma_{ns} = \phi^+_{np} - \phi^-_{sp}$, and the circulation associated with the ring bubble, $\phi^+_T - \phi^-_T$, versus time after initial impact, $t - T_c(Z_0)$, for various values of Z_0.

that found in (Best, 1993) where the circulation of the ring bubble is assumed to remain constant.

4 Conclusion

This study shows that the behavior of a cavitation bubble near a rigid wall is characterized by a process of a continuous re-entrant jet impact at the final stage of the collapse. During this process, the bubble is transformed into a toroidal-shaped cavity (ring bubble). This ring bubble is attached to an impact interface that represents a shear layer created by the impact. Before initial impact, the fluid in the re-entrant jet is moving toward the wall with high speed and the fluid on the other side of the bubble is moving away from the wall. During impact, a high-pressure region that is generated around the vortex sheet dramatically decelerates the fluid in the re-entrant jet and forces the fluid on the other side of the bubble to accelerate toward the wall.

5 Acknowledgments

SZ and JHD acknowledge the support of the state of Maryland and DYNAFLOW, INC. under a Maryland Industrial Partnership contract between the University of Maryland and DYNAFLOW, INC.

References

Best, J.: 1993, 'The formation of toroidal bubbles upon the collapse of transient cavities', *J. Fluid Mech.***Vol. 251**, pp. 79–107

Best, J. P. & Kucera, A.: 1992, 'A numerical investigation of non-spherical rebounding bubbles', *J. Fluid Mech.***Vol. 245**, pp. 137-154

Blake, J. R., Taib, B.B. & Doherty, G.: 1986, 'Transient cavities near boundaries. Part I. Rigid boundary', *J. Fluid Mech.***Vol. 170**, pp. 479-497

Chahine, G. L. & Perdue, T. O.: 1988, 'Simulation of the three-dimensional Behavior of an Unsteady Large Bubble near a Structure', *Drops and Bubbles, Third International Colloquium*, Monterey, CA., Ed. Taylor G. Wang, pp. 188–199

Duncan, J. H. & Zhang, S.: 1991, 'On the interaction of a collapsing cavity and a compliant wall', *J. Fluid Mech.***Vol. 226**, pp. 401-423

Kimoto, H.: 1987, 'An experimental evaluation of the effects of a water microjet and a shock wave by a local pressure sensor', *International Symposium on Cavitation Research Facilities and Techniques*, ASME, FED - **Vol 57**, pp. 217 - 224

Shima, A., Takayama, K. & Tomita, Y.: 1983, 'Mechanisms of impulsive pressure generation from spark-generated bubble collapse near a wall', *AIAA Journal.***Vol. 21, No. 1**, pp. 55-59

Tomita, Y. & Shima, A.: 1986, 'Mechanisms of impulsive pressure generation and damage pit formation by bubble collapse', *J. Fluid Mech.***Vol. 169**, pp. 535-564

Vogel, A. Lauterborn, W. & Timm, R.: , 1989, 'Optical and acoustic investigations of the dynamics of laser-produced cavitation bubbles near a solid boundary', *J. Fluid Mech.***Vol. 206**, pp. 299–338

Zhang, S., Duncan, J. H. & Chahine, G. L.: 1993, 'The final stage of the collapse of a cavitation bubble near a rigid wall", *J. Fluid Mech.* **Vol. 257**, pp. 147–181